PERGAMON

Deep-Sea Research II 49 (2002) 1197–1210

DEEP-SEA RESEARCH
PART II

www.elsevier.com/locate/dsr2

Annual Rossby waves in the Arabian Sea from TOPEX/POSEIDON altimeter and in situ data

Peter Brandt[a,*], Lothar Stramma[a], Friedrich Schott[a], Jürgen Fischer[a], Marcus Dengler[a], Detlef Quadfasel[b]

[a] *Institut für Meereskunde an der Universität Kiel, Düsternbrooker Weg 20, 24105 Kiel, Germany*
[b] *Niels Bohr Institutet for Astronomi, Fysik og Geofysik, Københavns Universitet, Juliane Maries Vej 30, 2100 Copenhagen, Denmark*

Accepted 30 September 2001

Abstract

Sea-surface height data acquired by the TOPEX/POSEIDON satellite over the Arabian Sea from October 1992 to October 1998 are analyzed. Strong seasonal fluctuations are found between 6° and 10°N, which are mainly associated with westward propagating annual Rossby waves radiated from the western side of the Indian subcontinent and that are continuously forced by the action of the wind-stress curl over the central Arabian Sea. An analysis of hydrographic data acquired during August 1993 and during January 1998 at 8°N in the Arabian Sea reveals the existence of first- and second-mode annual Rossby waves. These waves, which can be traced as perturbations in the density fields, have wavelengths of 12×10^3 and 4.4×10^3 km as well as phase velocities of 0.38 and 0.14 m/s, respectively. The waves are associated with a time-dependent meridional overturning cell that sloshes water northward and southward. Between 58° and 68°E in the central Arabian Sea, we found a Rossby-wave induced transport in the upper 500 m of about 10 Sv southward in August 1993 and northward in January 1998. Below 2000 m, there was still a northward transport of 3.2 Sv in August 1993 and a southward transport of 4.8 Sv in January 1998. A comparison of steric height differences between August 1993 and January 1998 calculated from the observed density fields as well as calculated from the reconstructed density fields using first- and second-mode annual Rossby waves agree quite well with the corresponding sea-surface height differences. Implications resulting from the reflection of annual Rossby waves, like fluctuations of the western boundary currents, are discussed.

1. Introduction

The seasonal cycle of the monsoon circulation in the Arabian Sea is characterized by vigorous changes of the Somali Current at its western margin (e.g. Schott and McCreary, 2001), while in the interior of the Arabian Sea the monsoon related circulation variability is generally small. In winter, the Somali Current flows southward off Somalia, crossing the equator and is supplied by inflow through the passage between Socotra and the African continent in the north as well as out of the Arabian Sea from the east (Schott and Fischer, 2000). In summer, the most prominent circulation feature is the *Great Whirl* (GW), which develops seasonally in the 5°–10°N latitude range off northern Somalia after the onset of the summer monsoon and may last well into the transition

*Corresponding author. Tel.: +49-431-600-4105; Fax: +49-431-600-174101.
E-mail address: pbrandt@ifm.uni-kiel.de (P. Brandt).

0967-0645/02/$ - see front matter
PII: S0967-0645(01)00166-7

period and even continue underneath the developing surface circulation of the winter monsoon. From WOCE surveys it was found that the GW is an almost closed circulation cell during the late summer monsoon with very little exchange with the interior Arabian Sea. Interannual variability of the GW was found to be substantial. While in August 1993 the northern limit of the GW was located about 200 km south of the southern shelf of Socotra (Fischer et al., 1996), the GW of 1995 was banked up against Socotra (Schott et al., 1997).

While the GW is mainly forced by local winds or by the wind-stress curl over the interior Arabian Sea (Schott, 1983), remote effects propagating in from the west cost of India appear to be relevant. Bruce et al. (1994) described the elevation of the sea surface in January near India as the Laccadive High (LH), an anticyclonic gyre that develops off the southwest coast of India just north of the Laccadives. They found a westward translation of the LH by January, with a subsequent dissipation in midbasin. During the summer monsoon, the LH is replaced by a region of low sea level, the Laccadive Low (LL). Using a numerical model, McCreary et al. (1993) found a strong decrease in the shallowing and deepening of the upper-layer thickness west of India when switching off the Bay of Bengal winds and concluded that these features are primarily remotely forced from the Bay of Bengal. Other model studies also confirmed that the LH/LL are generated at least partially due to remote forcing out of the Bay of Bengal (Bruce et al., 1994; Shankar and Shetye, 1997).

Regarding the meridional overturning circulation and heat transport, the northern Arabian Sea is known to be a net heat exporter, with a large annual cycle superimposed such that in winter there is a net heat import into the northern hemisphere (Garternicht and Schott, 1997). The mechanism through which this seasonal reversal of the meridional heat transport occurs is to a large degree attributed to the seasonal reversal of the meridional Ekman transports, but vertical shear consisting largely of thermal wind shear balanced by zonal density gradients and a small ageostrophic shear also appear to contribute (Lee and Marotzke, 1998; Schott and McCreary, 2001).

In this presentation we study the seasonal difference of the density field along an 8°N section across the interior Arabian Sea, based on two hydrographic cruises, of summer 1993 and winter 1998. We will show that the structural difference of the density field, below the immediate surface-mixed layer, can be explained to a large extent by the superposition of a first- and a second-mode annual Rossby wave. For comparison we also analyze wave patterns from sea-surface height (SSH) data from TOPEX/POSEIDON altimetry and find good agreement with the modal analysis of the seasonal hydrographic sections. From the structure of the annual signal in the SSH data we argue that the annual signal is mainly composed of westward propagating annual Rossby waves that are radiated from the western side of the Indian subcontinent and that are continuously forced by the action of the wind-stress curl over the central Arabian Sea.

2. Data and methods

Three main data sets are used in this study: (1) altimeter-derived sea-surface height (SSH) anomaly data, (2) hydrographic in situ data, and (3) scatterometer-derived wind-stress curl data. The altimeter data, which are corrected for geophysical, tidal, sea state, and instrument effects as well as for orbit errors, are part of the TOPEX/POSEIDON sea-level anomaly products provided by CNES/NASA (AVISO, 1998). Here, we use SSH anomalies from along-track data (Fu et al., 1994) for the period of October 1992–October 1998 for comparison to ship sections and for information on the temporal changes of some signals. The data were processed as follows: After taking the median of the along-track data within evenly spaced 50-km bins, the resulting gridded median along track-data were interpolated by objective analysis to a $1^\circ \times 1^\circ$ grid. Amplitude and phase of the seasonal signal were determined by fitting an annual harmonic to the time series of the gridded median along-track data using minimum variance criteria. Finally also these data (amplitudes of annual sin and cos waves) were interpolated to a $1^\circ \times 1^\circ$ grid.

The hydrographic in situ data used in this study were acquired during the RV *Sonne* cruise 89 (SO89) in August 1993 and during RV *Sonne* cruises 128 (SO128) in January 1998 along the WOCE IR1W section at 8°N. Hydrographic profiles were collected with a Neil-Brown Mark III CTD-system. The calibration of the CTD data resulted for both cruises in accuracies of 0.002°C in temperature, 0.003 in salinity, and 4.5 dbar in pressure.

The wind data used in this study were acquired by the Scatterometer aboard the ERS-1/2 satellites. Here we use only the annual cycle of the wind-stress curl calculated from weekly wind data for the same period as the annual cycle of the SSH anomaly: from October 1992 to October 1998.

3. SSH anomaly and wind-stress curl

An efficient tool to study changes in the circulation pattern as well as Rossby wave dynamics is satellite altimetry as it provides basin-wide observations of the sea level. For example, Périgaud and Delecluse (1992) used Geosat satellite altimetry to study the annual SSH variations in the Indian Ocean. Basu et al. (2000) analyzed 4 years of TOPEX/POSEIDON altimeter data with respect to annual and interannual SSH variations. In both studies, satellite observations were compared with model simulations. Here, we will use altimetric SSH data to interpret density variations observed in the central Arabian Sea.

Fig. 1 shows the spatial distribution of amplitude and phase of the annual harmonic of SSH anomalies from TOPEX/POSEIDON altimetry as well as the percentage of total variance explained by the annual harmonic. From this figure, an annual signal in the Arabian Sea can be delineated as a band of enhanced amplitude in the latitude range 6°–10°N, with its maximum elevation in January near India and in June near Africa. In this area, the annual signal is the dominant signal in the SSH anomaly. In the central Arabian Sea, it explains more than 60% of the total variance of the SSH anomaly. This band of enhanced amplitude was interpreted by Subrahmanyam et al. (2001) as first- and second-mode Rossby waves propagating westward from the western side of the Indian subcontinent towards Africa. However, there is also a local maximum in the band of enhanced amplitude of the annual harmonic of SSH anomaly at about 60°E (see Fig. 1a), which cannot be explained by the radiation of free Rossby waves from the eastern boundary as these waves must gradually decay during their propagation (Qiu et al., 1997). The most likely candidate causing this local maximum is the wind-stress curl. Fig. 2 shows the spatial distribution of amplitude and phase of the annual harmonic of the wind-stress curl as measured by the ERS Scatterometer as well as the percentage of total variance explained by the annual harmonic. The annual signal in the wind stress curl is dominant only in the southwestern part of the Arabian Sea. There, the maximum negative wind-stress curl is found in July caused by the strong winds of the Southwest Monsoon. The action of the wind leads, in general, to the generation of first- and second-mode Rossby waves. In particular, Masumoto and Meyers (1998) found for the southern tropical Indian Ocean that the Ekman pumping on a large scale strongly modifies Rossby waves radiating from the eastern boundary. They found distinct maxima in the amplitude at a given latitude resulting from a continuous forcing of Rossby waves by the wind-stress curl, the number of maxima being dependent on the longitudinal distance from the eastern boundary, and on the phase speed of nondispersive, long Rossby wave. Analogously the annual Rossby waves in the Arabian Sea should not be seen as a free Rossby wave simply radiating from the western side of the Indian subcontinent, but as Rossby waves that are continuously forced by the wind-stress curl over the central Arabian Sea. This may explain the occurrence of the local maximum in the amplitude of the annual harmonic of SSH anomaly.

A longitude-time plot of the SSH anomaly at 8°N for the period October 1992–October 1998 is shown in Fig. 3. This figure reflects mainly the annual cycle of westward propagating SSH elevations and depressions generated near India during each year along 8°N. However, there are considerable smaller scale signals of monthly to two

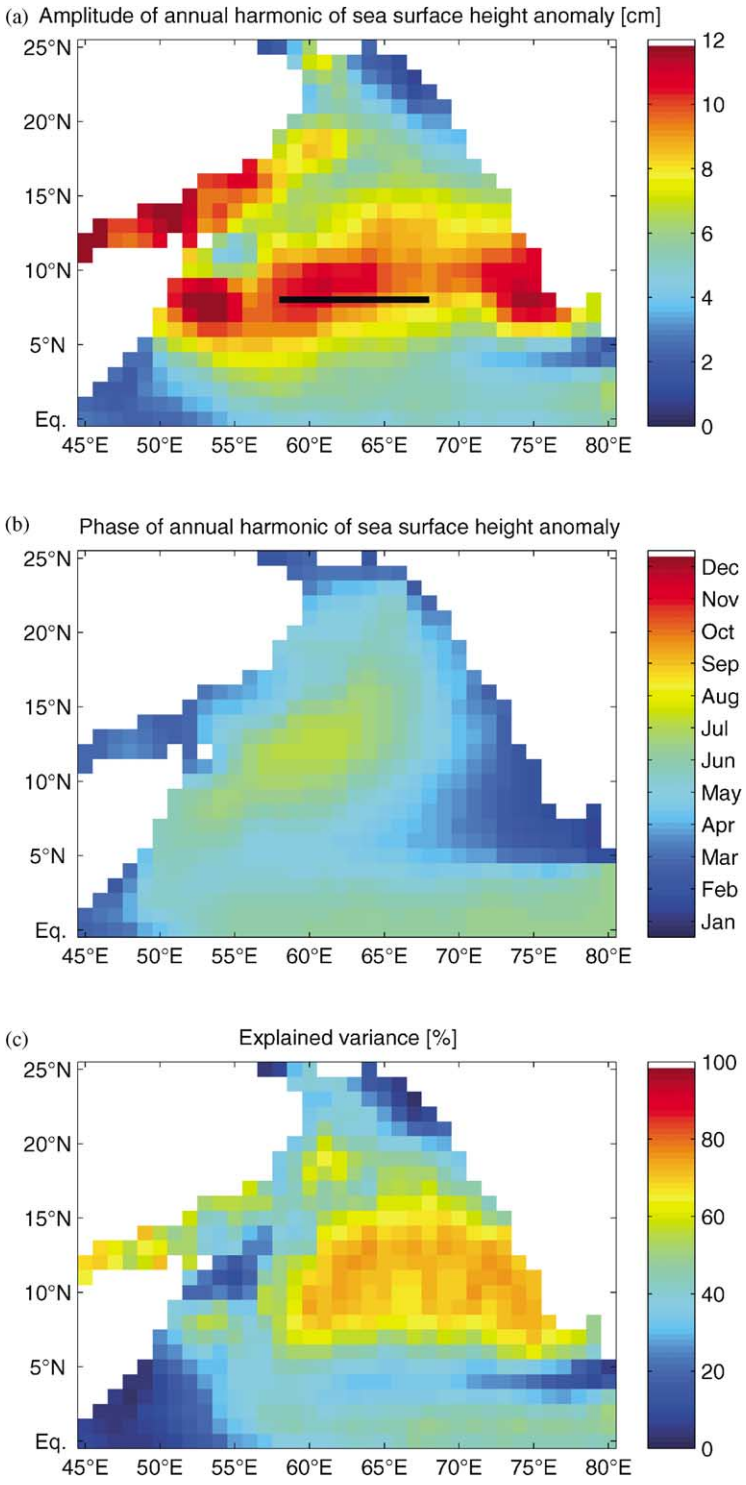

Fig. 1. Amplitude of the annual cycle of the TOPEX/POSEIDON SSH. anomaly (a), month of its maximum elevation (b), and percentage of total variance contained in the annual cycle (c). The black line in (a) gives the location of the density sections analyzed in the following. The hydrographic data were acquired during two cruises by RV *Sonne* in August 1993 (SO89) and in January 1998 (SO128).

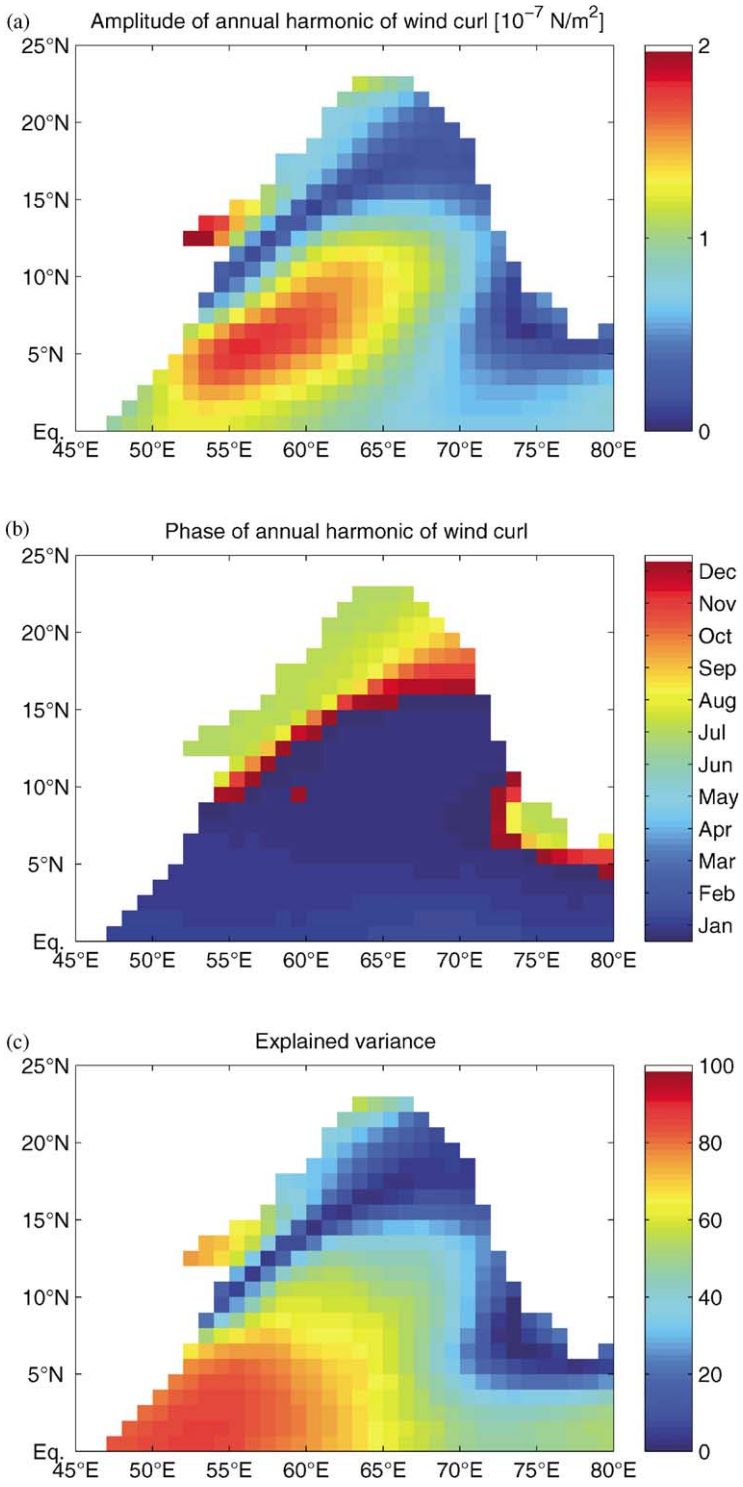

Fig. 2. Amplitude of the annual cycle of the ERS wind-stress curl (a), month of its maximum strength (b), and percentage of total variance contained in the annual cycle (c).

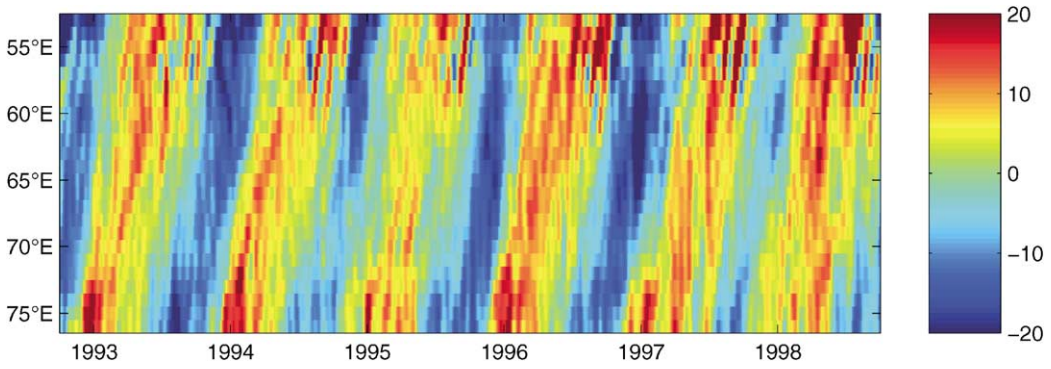

Fig. 3. Longitude-time plot of TOPEX/POSEIDON SSH anomaly (cm) at 8°N.

monthly periods that propagate westward superimposed on the annual signal. On the one hand, these signals seem to originate from the west coast of India and are partly damped in the interior of the Arabian Sea, on the other, these signals are strongly amplified near the African coast. In the latter region Dengler et al. (2002) also observed strong fluctuations in the velocity field measured by moored current meters. These strong fluctuations near the African coast are probably connected to the evolution of the Great Whirl generated with the onset of the Southwest Monsoon in May. In this investigation we want to focus on the annual signal that, as will be shown in the next section, can be also found in the hydrographic sections along 8°N.

4. Hydrographic sections

In this section, hydrographic data acquired at the 8°N section during the two *Sonne* cruises in August 1993 and January 1998 will be analyzed only for the central part of the Arabian Sea. This restriction was necessary to avoid that strong circulation features like the Great Whirl on the western side of the Arabian Sea or the LH/LL on the eastern side of the Arabian Sea disturb our analysis with respect to annual Rossby waves. The chosen section extends from 58° to 68°E at 8°N in the central Arabian Sea. Fig. 4 shows the observed density difference for August 1993 compared to January 1998 at this section. In this figure, a positive density anomaly in the upper 50 m of the water column can be observed, which results from the presence of different water masses in the near-surface layer during the different seasons: While in August, the near-surface layer is occupied by salinity-rich Arabian Sea Water, in January, salinity-poor water from the Bay of Bengal is transported into the Arabian Sea by the Northeast Monsoon Current. However, there are two striking features visible in the field of density difference that cannot be explained by seasonal variations in the water mass properties: (1) a negative density anomaly in the depth range 50–1000 m shallower in the eastern part, and (2) a positive density anomaly underneath. In the following, we will show that these two features can mainly be attributed to the vertical displacement of the pycnoclines due to westward propagating Rossby waves of annual period.

Fig. 5 shows the square of the Brunt–Väisälä frequency, N^2, and the first two displacement modes. The Brunt–Väisälä frequency profile is calculated from a mean density profile that is derived by averaging the density profiles of both cruises separately and then averaging the resulting two profiles. It is transformed into vertical displacement modes, which define an orthonormal system, by solving the vertical structure equation. The eigenvalues of the solution define the phase velocity of internal gravity waves, c_n. In the following, we use the density perturbation modes that are calculated by multiplying the displacement modes with N^2. To estimate the wavelength of annual Rossby waves, we use the following approximation of the dispersion relation of

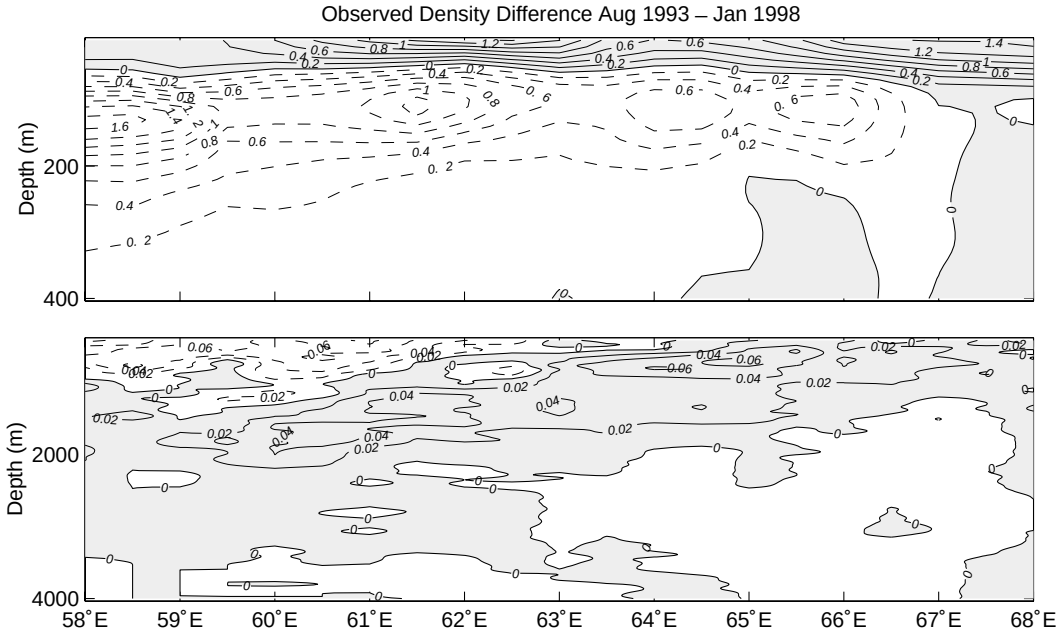

Fig. 4. Observed difference in density (kg/m^3) for August 1993 compared to January 1998 (positive differences represent higher values in August 1993) for the central part of the 8°N section across the Arabian Sea. In the upper panel, the density differences in the upper 400 m are shown, in the lower panel, the density difference from 400 to 4000 m water depth with different contour intervals. The plotted data are vertically low-pass filtered; the low-pass wave number is 0.01 m^{-1}.

Rossby waves, which in general is valid for long Rossby waves:

$$\omega = \beta k_n R_n^2, \tag{1}$$

where ω and k denote the Rossby wave frequency and wave number, respectively, $R_n = c_n/f$ the internal Rossby radius of deformation, f the Coriolis parameter, and β the meridional gradient of f. The resulting values of wavelength $\lambda_n = 2\pi/k_n$, phase velocity $c_{rn} = \omega/k_n$ of annual Rossby waves as well as the internal Rossby radius are given in Table 1. The wavelengths of the first- and second-mode Rossby waves are larger than the width of the Arabian Sea, i.e. only a small portion of the wavelength fits into the area of investigation.

Modal amplitudes are calculated by projecting each individual measured density profiles onto the density perturbation modes. Fig. 6 shows the amplitude distribution for the first two density perturbation modes for density profiles acquired between 58° and 68°E in August 1993 during SO89 and in January 1998 during SO128. Also shown in this figure are fits that represent linear Rossby waves of the form:

$$A = A_0 \cos(k_n x + \phi), \tag{2}$$

where A_0 and ϕ denote the amplitude and phase of the Rossby wave, and x the horizontal coordinate ($x = 0$ at 68°E) negative to the west. Fitted are the amplitudes and phases of the Rossby waves by means of a least-squares minimization. The numbers obtained are given in the figure. The amplitudes derived from both sections are very similar for first as well as second-mode waves and the phases show a nearly 180° phase difference between August 1993 and January 1998, which is not inconsistent with our assumption that variations in the density field mainly arise from Rossby waves of annual period. Using the calculated amplitudes and phases of the first two density perturbation modes, the density fields can be reconstructed. Fig. 7 shows the reconstructed density difference for August 1993 compared to January 1998. By comparing this figure with Fig. 4 one can conclude that while the positive

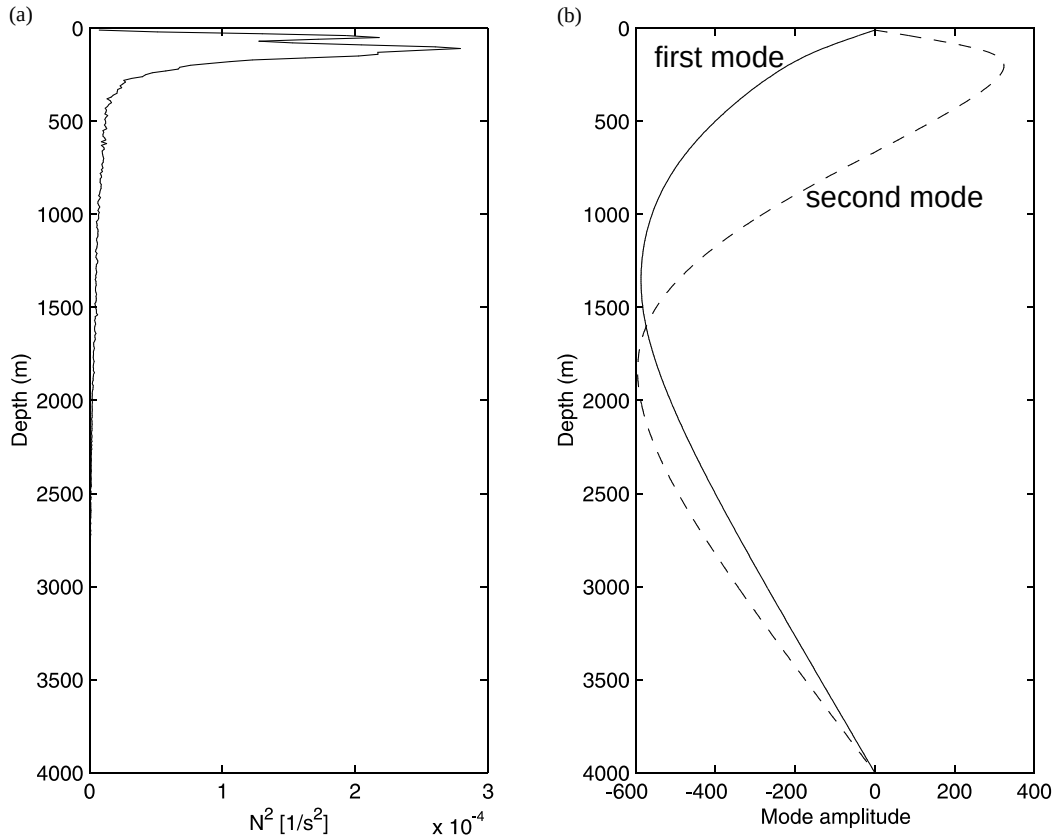

Fig. 5. Mean Brunt–Väisälä frequency (a) and first (solid line) and second (dashed line) displacement mode (b) as calculated from the mean density profile of hydrographic data acquired in August 1993 and in January 1998 at 8°N between 58° and 68°E in the central Arabian Sea.

Table 1
Parameters of first- and second-mode annual Rossby waves in the Arabian Sea at 8°N

Parameter	Notation	$n=1$	$n=2$
Wavelength	λ_n 10^3 (km)	12	4.4
Phase velocity	c_{rn} (m/s)	0.38	0.14
Internal Rossby radius	R_n (km)	130	79

near-surface density anomaly cannot be explained by annual Rossby waves as expected, the signals in the observed density difference below the near-surface layer are well represented by signals in the reconstructed density difference. Looking at the whole water column, the reconstructed field of density difference explains 58% of total variance. When excluding the upper 100 m of the water column it explains even 87% of total variance.

Fig. 8 shows the geostrophic velocities as calculated from the reconstructed density fields for August 1993 and January 1998. The velocities of both modes are nearly reversed from August 1993 to January 1998 and are of similar magnitude. The near-surface velocities reaching about 2 and 4 cm/s for the first- and second-mode Rossby wave, respectively, resulting in a maximum near surface velocity of about 6 cm/s to the south in August 1993 and to the north in January 1998. By integrating the velocity over the whole section from 58° to 68°E, cumulative transports can be calculated by integrating vertically upward (Fig. 9). As only baroclinic modes are involved in the analysis no net water gain or loss is possible

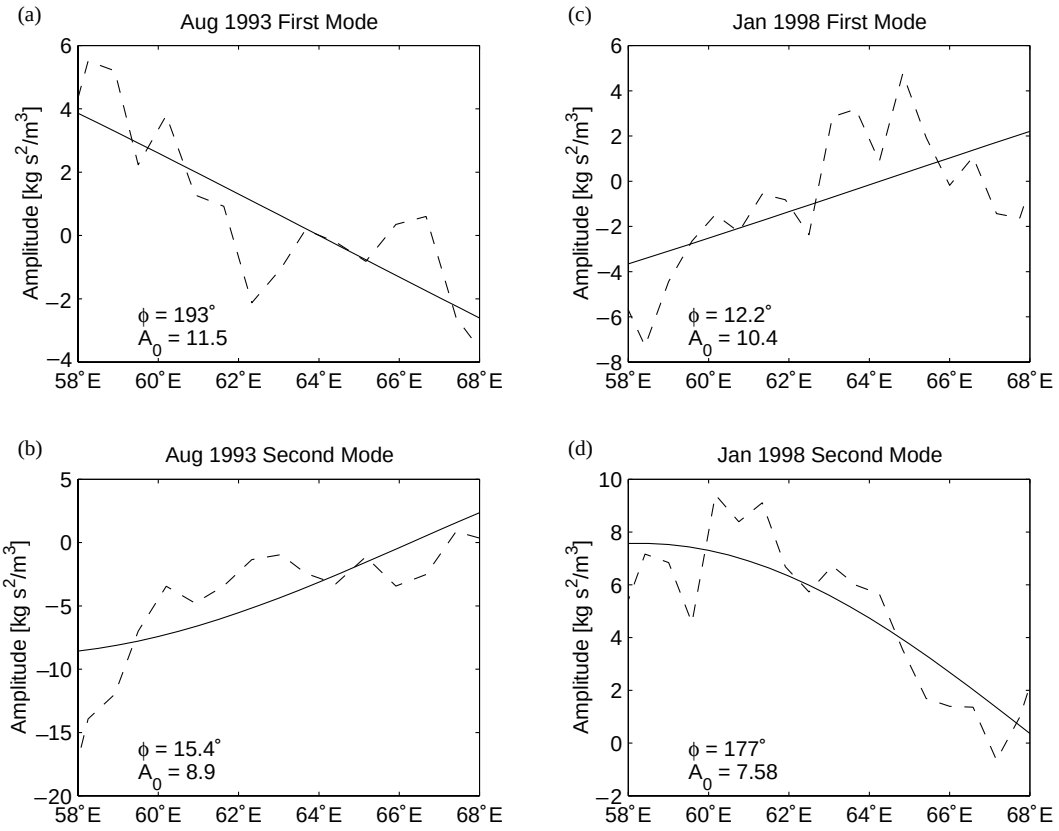

Fig. 6. Amplitude distribution obtained from the modal decomposition (dashed lines) for the first mode (a) and (c) and for the second mode (b) and (d). Also included is a least-square fit according to Eq. (2). The density perturbation relative to a mean density profile can be reconstructed by multiplying the displayed amplitudes with the corresponding displacement mode times N^2 (see Fig. 5).

due to the described Rossby waves. The propagation of the first- and second-mode Rossby waves results in a seasonally reversing baroclinic transports that slosh water northward and southward. While the transport in the upper 500 m of the water column of about 10 Sv is directed southward in August 1993, it is directed northward in January 1998. Below 2000 m, there is still a northward transport of 3.2 Sv in August 1993 and a southward transport of 4.8 Sv in January 1998.

5. Discussion and conclusion

A comparison between altimetric signals and observed density fields can be performed by calculating steric height variations out of the density fields. Using the observed density fields the corresponding steric height can be calculated as follows:

$$\eta_{\mathrm{sh}} = \frac{1}{\rho_0}\int_{-D}^{0} \rho'(z)\,\mathrm{d}z, \tag{3}$$

where $\rho' = \rho - \rho_0$ denotes the time-dependent density anomaly relative to the mean density profile. Here, the depth D denotes the depth of the sea bottom. Calculating the SSH according to Eq. (3) summarizes the effects of near surface density anomalies and of density changes below the seasonal thermocline due to changing currents, but it neglects the effect of the barotropic current field (see, e.g., Stammer, 1997). The last effect is, in general, small in the region of investigation. Fig. 10 shows a comparison of the observed steric

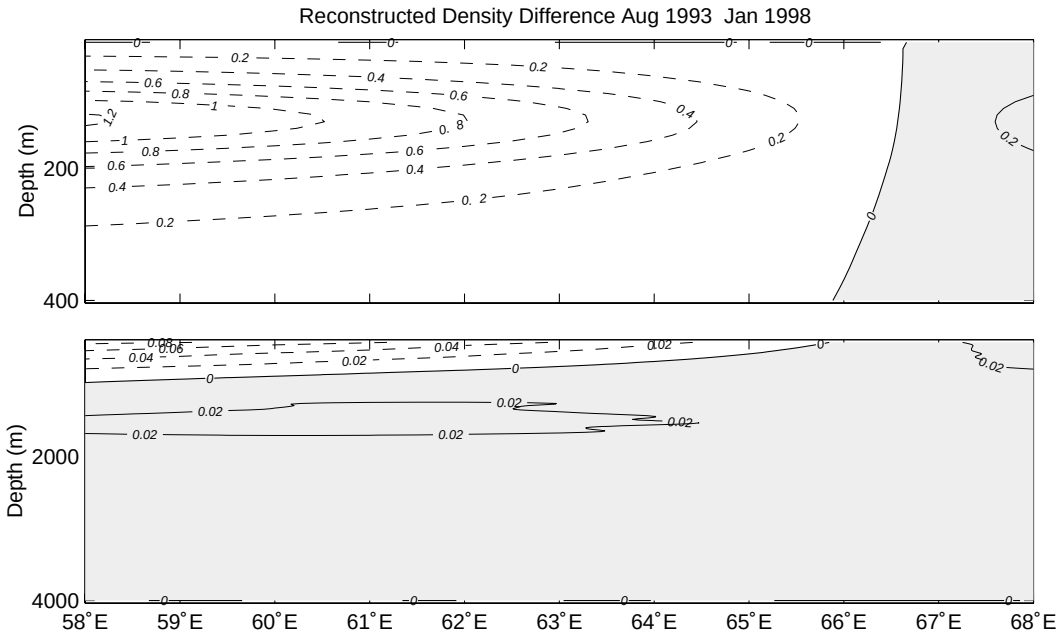

Fig. 7. Difference in density (kg/m^3) for August 1993 compared to January 1998 (positive differences represent higher values in August 1993) for the central part of the 8°N section across the Arabian Sea as reconstructed from the first two density perturbation modes. In the upper panel, the density difference in the upper 400 m is shown, in the lower panel the density difference from 400 to 4000 m water depth with different contour intervals. The plotted data are vertically low-pass filtered; the low pass wave number is 0.01 m^{-1}.

height difference between August 1993 and January 1998 and the corresponding difference in the SSH anomaly. Also shown are the steric height differences as calculated from the reconstructed density fields of the first- and second-mode annual Rossby wave as well as the sum of both. While the mean slope of steric height difference for both, first- and second-mode Rossby waves, is smaller than the corresponding slope of the SSH difference, the mean slope of the sum of both modes as well as the mean slope of the observed steric height difference agree quite well with the slope of the observed SSH difference. That means the seasonal variations in the SSH of the central Arabian Sea at 8°N (see Fig. 1) can be mainly attributed to the westward propagation of first- and second-mode annual Rossby waves. This result agrees well with the result obtained recently by Subrahmanyam et al. (2001). They identified the main peaks in the energy spectrum of the SSH of the central Arabian Sea measured by the TOPEX/POSEIDON altimeter as well as simulated by a numerical model as first- and second-mode Rossby waves. The source of these Rossby waves can be traced back at least partially to the LH/LL at the western side of Indian subcontinent. However, the annual cycle of the wind-stress curl over the central Arabian Sea act to modify the propagating Rossby waves. In particular, the western maximum in the amplitude of the annual harmonic of the SSH (Fig. 1) cannot be explained by the radiation of free Rossby waves from the LH/LL as these waves must gradually decay during their propagation (Qiu et al., 1997). It is most likely connected to the continuous forcing of the Rossby waves by the wind-stress curl over the central Arabian Sea. As shown by Schott and Quadfasel (1982), the sudden onset of offshore currents in the northern Somali Current region after the summer monsoon onset 1979 could be identified as Rossby wave response to the offshore wind-stress curl. However, the continuous forcing by the wind-stress curl as well as the decay of the annual Rossby waves in the Arabian Sea leads, in general, to Rossby wave parameters that are

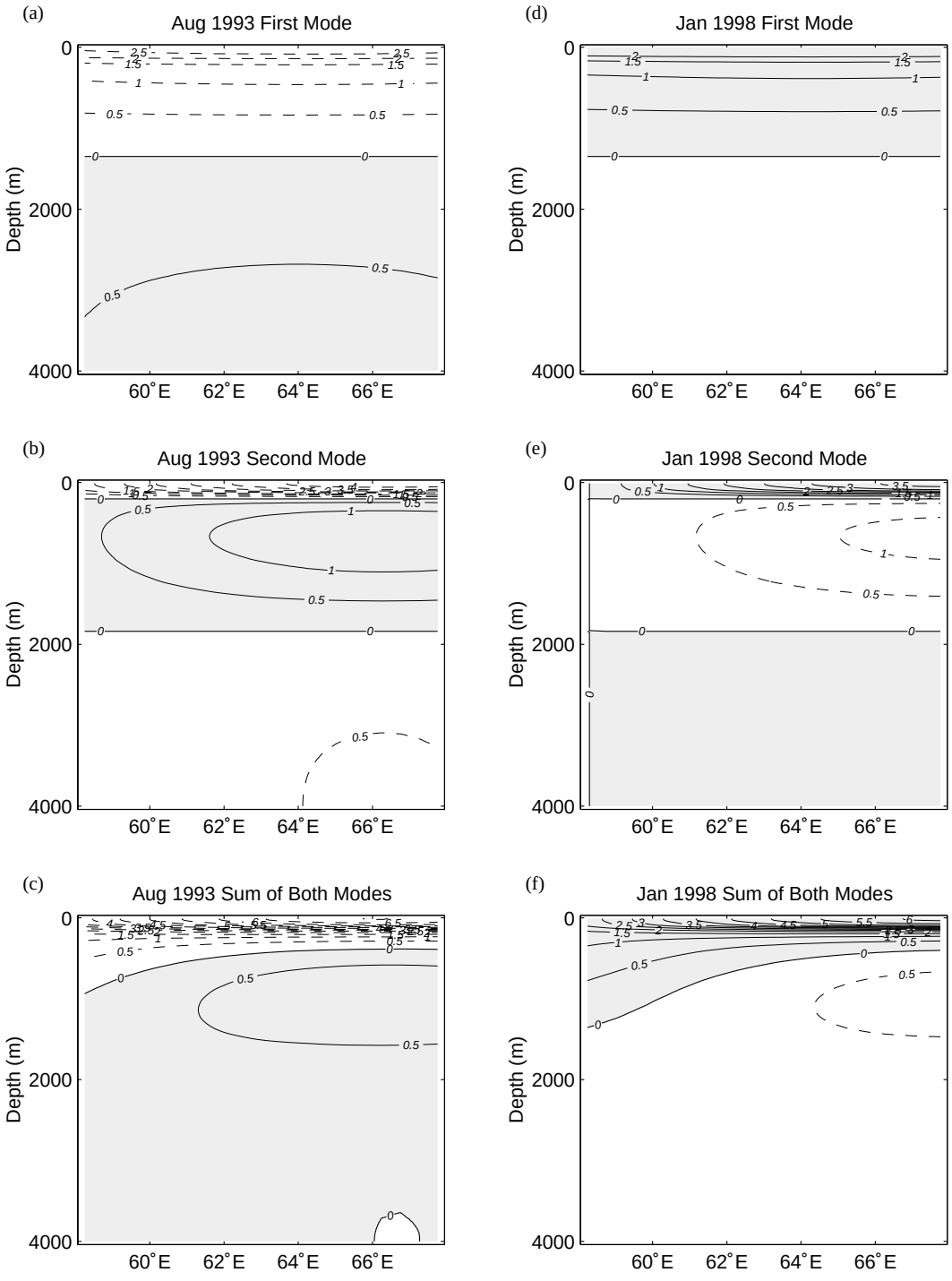

Fig. 8. Geostrophic velocities (cm/s) as calculated from the reconstructed density fields of the first mode (a) and (d), the second mode (b) and (e), and the sum of both modes (c) and (f) for August 1993 (left panels) and January 1998 (right panels).

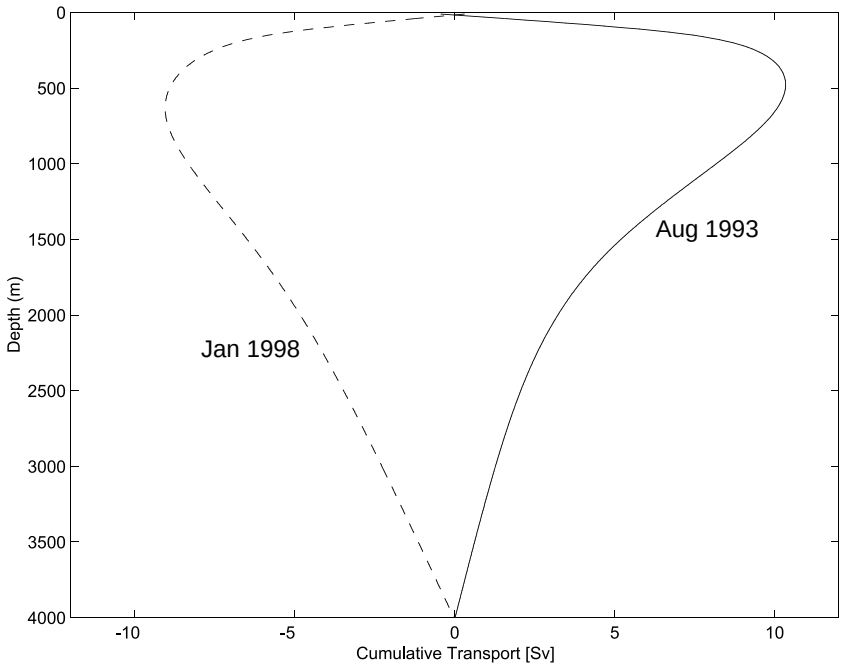

Fig. 9. Cumulative transports as integrated between 58° and 68°E and from the bottom to the sea surface for August 1993 (solid line) and January 1998 (dashed line).

dependent on longitude. This dependence is neglected in our analysis when fitting the shapes of first- and second-mode Rossby waves to the amplitude distribution for the corresponding density perturbation modes. The fitted Rossby wave solutions thus may not represent exactly the actual combined forced and free Rossby waves in the Arabian Sea. Nevertheless they describe to a high degree the observed density fields that determine the geostrophic velocity fields.

In fact, the propagation of the obtained first- and second-mode annual Rossby waves results in seasonally reversing baroclinic transports that slosh water northward and southward. The transport due to the annual Rossby waves at 8°N between 58° and 68°E in the upper 500 m of the water column is about 10 Sv to the south in August 1993 and about 10 Sv to the north in January 1998. Below 2000 m, there was still a northward transport of 3.2 Sv in August 1993 and a southward transport of 4.8 Sv in January 1998. Thus the annual Rossby waves generate the appearance of time-dependent meridional overturning cells superimposed on pre-existing stationary meridional overturning cells (see, e.g., Lee and Marotzke, 1998; Schott and McCreary, 2001; Stramma et al., 2002).

Long Rossby waves that encounter the western boundary will reflect into short Rossby waves. These short waves act only to redistribute mass along the coast (e.g. Cane and Gent, 1984; Visbeck and Schott, 1992). In the near-surface layer, the resulting seasonally varying western boundary currents represent only small contributions to the strong variability in the existing current field, e.g., connected with the Great Whirl, although they may play a significant role in the formation and the decay of this eddy. However, observed seasonal velocity fluctuations in the deep western boundary regime (Beal et al., 2000; Dengler et al., 2002) are probably associated with the reflection of long Rossby waves of annual period. The zonal and vertical structure of the time-dependent boundary currents resulting from the reflection of long Rossby waves can be very complicated. It depends on the exact superposition of Rossby

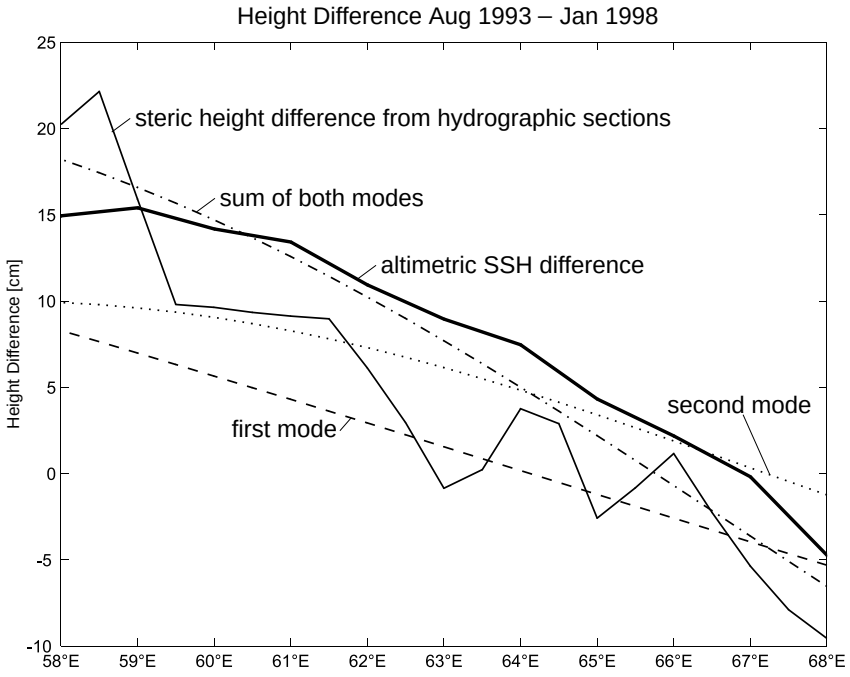

Fig. 10. Steric height difference between August 1993 and January 1998 as calculated by integration from bottom to surface of the observed density field (solid line) as well as of the reconstructed density fields. Steric height difference of the first mode is denoted by a dashed line, of the second mode by a dotted line, and of the sum of both modes by a dashed–dotted line. Also included is the SSH difference as observed from altimetry (thick solid line).

waves of different vertical modes as well as on their arrival time at the eastern boundary, which is additionally a function of latitude. However, such fluctuation can be understood at least partially as being remotely forced out of the Bay of Bengal via the LH/LL at the western side of the Indian subcontinent.

Acknowledgements

We express our gratitude to CNES/NASA and AVISO/Altimetry for provision of TOPEX/POSEIDON "SLA" altimeter data and to IFREMER for provision of wind data. We thank the captain and crew of the RV *Sonne* for their help, A. Rubino for helpful discussions, and C. Meinke for technical assistance. Financial support was obtained by the Bundesminister für Bildung und Forschung, Bonn, Germany under grants 03F157A, 03F0246A, 03R430 and 03G0128A.

References

AVISO, 1998. AVISO User Handbook for Sea Level Anomalies (SLA's), AVI-NT-011-312-CN, Edition 3.1. CLS Space Oceanography Division, Toulouse, France, 24 pp.

Basu, S., Meyers, S.D., O'Brien, J.J., 2000. Annual and interannual sea level variations in the Indian Ocean from TOPEX/POSEIDON observations and ocean model simulations. Journal of Geophysical Research 105, 975–994.

Beal, L.M., Molinari, R.L., Chereskin, T.K., Robbins, P.E., 2000. Reversing bottom circulation in the Somali Basin. Geophysical Research Letters 27, 2565–2568.

Bruce, J.G., Johnson, D.R., Kindle, J.C., 1994. Evidence for eddy formation in the eastern Arabian Sea during northeast monsoon. Journal of Geophysical Research 99, 7651–7664.

Cane, M.A., Gent, P.R., 1984. Reflection of low-frequency equatorial waves at arbitrary western boundaries. Journal of Marine Research 42, 487–502.

Dengler, M., Quadfasel, D., Schott, F., 2002. Abyssal circulation in the somali basin. Deep-Sea Research 49, 1297–1322.

Fischer, J., Schott, F., Stramma, L., 1996. Currents and transports of the great Whirl—Socotra gyre system during the summer monsoon August 1993. Journal of Geophysical Research 101 (C2), 3573–3587.

Fu, L.-L., Christensen, E.J., Yamarone, C.A., Lefebvre, M., Menard, Y., Dorrer, M., Escudier, P., 1994. TOPEX/POSEIDON mission overview. Journal of Geophysical Research 99, 24369–24381.

Garternicht, U., Schott, F., 1997. Heat fluxes in the Indian Ocean from a global eddy-resolving model. Journal of Geophysical Research 102, 21147–21159.

Lee, T., Marotzke, J., 1998. Seasonal cycles of meridional overturning and heat transport of the Indian Ocean. Journal of Physical Oceanography 28, 923–943.

Masumoto, Y., Meyers, G., 1998. Forced Rossby waves in the southern tropical Indian Ocean. Journal of Geophysical Research 103, 27589–27602.

McCreary, J.P., Kundu, P.K., Molinari, R.L., 1993. A numerical investigation of dynamics, thermodynamics and mixed-layer processes in the Indian Ocean. Progress in Oceanography 31, 181–244.

Périgaud, C., Delecluse, P., 1992. Annual sea level variations in the southern tropical Indian ocean from Geosat and shallow-water simulations. Journal of Geophysical Research 97, 20169–20178.

Qiu, B., Miao, W., Müller, P., 1997. Propagation and decay of forced and free baroclinic Rossby waves in off-equatorial oceans. Journal of Physical Oceanography 27, 2405–2417.

Schott, F., 1983. Monsoon response of the Somali Current and associated upwelling. Progress in Oceanography 12, 357–381.

Schott, F., Fischer, J., 2000. Winter monsoon circulation of the northern Arabian Sea and Somali Current, 1995. Journal of Geophysical Research 105, 6359–6376.

Schott, F., McCreary, J., 2001. The monsoon circulation of the Indian Ocean. Progress in Oceanography 51, 1–123.

Schott, F., Quadfasel, D., 1982. Variability of the Somali Current system during the onset of the Southwest Monsoon, 1979. Journal of Physical Oceanography 12, 1343–1357.

Schott, F., Fischer, J., Garternicht, U., Quadfasel, D., 1997. Summer monsoon response of the northern Somali Current, 1995. Geophysical Research Letters 24, 2565–2568.

Shankar, D., Shetye, S.R., 1997. On the dynamics of the Lakshadweep high and low in the southeastern Arabian Sea. Journal of Geophysical Research 102, 12551–12562.

Stammer, D., 1997. Steric and wind-induced changes in TOPEX/POSEIDON large-scale sea surface topography observations. Journal of Geophysical Research 102, 20987–21009.

Stramma, L., Brandt, P., Schott, F., Quadfasel, D., Fischer, J., 2002. Winter and summer monsoon water mass, heat and fresh water transport changes in the Arabian Sea near 8°N. Deep-Sea. Research II 49, 1173–1195.

Subrahmanyam, B., Robinson, I.S., Blundell, J.R., Challenor, P.G., 2001. Indian Ocean Rossby waves observed in TOPEX/POSEIDON alimeter data and in model simulations. International Journal of Remote Sensing 22, 141–167.

Visbeck, M., Schott, F., 1992. Analysis of seasonal variations in the western equatorial Indian Ocean: direct measurements and GFDL model comparison. Journal of Physical Oceanography 22, 1112–1128.